Auger recombination in GaAs and GaSb†

G. Benz* and R. Conradt
Physikalisches Institut der Universität Stuttgart, Pfaffenwaldring 57, D-7000 Stuttgart-80, Federal Republic of Germany
(Received 4 June 1976)

In highly excited GaAs and GaSb luminescence bands above the band gap at $h\nu = E_g + \Delta_0$ are observed, which are explained by radiative recombination of Auger-excited holes in the split-off valence band with free or shallow bound conduction-band electrons. An extremely weak luminescence continuum in both materials between $h\nu = E_g$ and $h\nu = 2E_g$, which shows no distinct structure within the experimental resolution, is ascribed to the radiative recombination of relaxing Auger electrons in the conduction band. The role of the split-off valence band for hole-hole-electron (hhe) Auger recombination is explained. From spectroscopic data the hhe Auger coefficients C_p for GaAs $[C_p(\mathrm{GaAs})_{77\,\mathrm{K}} \approx 10^{-(31\pm1)}\ \mathrm{cm^6 sec^{-1}}]$ and for GaSb $[C_p(\mathrm{GaSb})_{77\,\mathrm{K}} \approx 10^{-(25\pm1)}\ \mathrm{cm^6 sec^{-1}}]$ are estimated, in rough agreement with theoretically predicted values. The dependence of the luminescence intensities of the investigated emission bands in GaSb at E_g and at $E_g + \Delta_0$ on the exciting light density and on the doping concentration leads to the conclusion that in p-type GaSb band-to-band Auger recombination occurs. The surprisingly high intensity of the emission, which is connected with a hhe Auger process, in n-type GaSb(Te) and its strange dependence on the excitation power is explained by a band-to-acceptor Auger process. It is believed that this acceptor is the doubly ionizable native defect in GaSb, which is always present.

I. INTRODUCTION

As an explanation of radiationless recombination in semiconductors at high carrier densities and transition energies that are greater than the energy of phonons, the Auger recombination usually is considered. Most of the theoretical and experimental work done in this field is summarized in some review articles.[1-4] The practical significance of the Auger recombination lies in the fact that it limits the charge-carrier lifetime at high carrier densities. This is of increasing importance for semiconductor devices in heavy-current engineering.[5]

The Auger recombination is a process of third-order reaction kinetics. Mostly, an experimental proof of the Auger recombination is performed indirectly by studying the reaction kinetics of the recombination. In doing so, the dependence of the charge-carrier lifetime[6] or of the luminescence quantum efficiency[7] on the carrier density was measured. Pancove *et al.*[8] succeeded in getting indication of the Auger electrons emitted from a cesium-coated GaAs surface. Conradt[9] and Betzler[10] identified the Auger carriers in Ge and Si by measuring the luminescence signal, arising from radiative transitions succeeding the Auger recombination.

In an Auger process, the energy released by the recombination of an electron-hole pair is transferred to a second electron or to a second hole, which are energetically lifted within their band or into another band. The Auger carriers dissipate this energy by emission of phonons. During the energy relaxation, a radiative recombination of these carriers with thermalized ones in the opposite band is possible. This gives rise to an extremely weak luminescence spectrum above the band gap.

In this paper we report luminescence measurements above the band gap, performed on the III-V compounds GaAs and GaSb. Preliminary results obtained from GaSb have been presented in an earlier letter.[11] Because of its band structure, GaSb should be a good model for studying the Auger recombination. The transition probability for a phononless Auger process[12] depends on the momentum transfer Δk of the impact partners as Δk^{-4}. Furthermore, if momentum conservation is presumed, an activation energy of the carriers is necessary.[12,13]

In GaSb the energy gap, $E_g = 0.812$ eV,[14] is nearly equal to the spin-orbit splitting of the valence bands $\Delta_0 \simeq 0.749$ eV.[15] As Fig. 1(a) depicts, in this band structure the hole-hole-electron (hhe) Auger process generating holes in the split-off valence

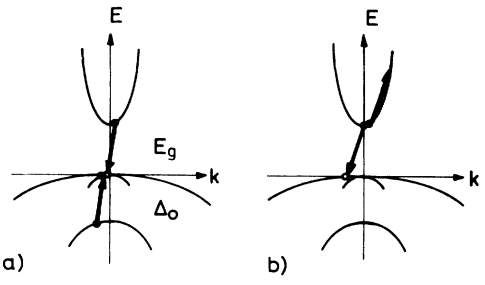

FIG. 1. Auger recombination in GaSb (schematic graph) with (a) hhe process and (b) eeh process.

band is possible with small momentum transfer and small activation energy and, therefore, with great transition probability.[16,17] This mechanism can be investigated by measuring the luminescence signal at $h\nu = E_g + \Delta_0$, which is caused by the radiative recombination of the Auger-excited holes in the split-off valence band with thermalized conduction-band electrons. In contrast to the hhe Auger process, the electron-electron-hole (eeh) mechanism [see Fig. 1(b)] will lead to a broad luminescence continuum from $h\nu = 2E_g +$ activation energy to $h\nu = E_g$.

A further peculiarity of GaSb is the fact that it always contains a native lattice defect[18,19] (combination of a Ga vacancy and a Ga atom on Sb site) which acts as a doubly ionizable acceptor. Since the acceptor can bind two localized holes, the recombination at this center should have a large probability for Auger recombination.[20] At high concentrations of the native acceptor a strong "Auger signal" should result. This band-to-acceptor Auger mechanism will be discussed in connection with compensated GaSb(Te).

The results, which will be described firstly, are obtained from GaAs samples. The band structure data of GaAs are disadvantageous to Auger processes involving the split-off valence band ($E_g = 1.519$ eV compared with $\Delta_0 = 0.341$ eV).[21,22] The expected lower hhe Auger transition rate in GaAs will be compared with the results obtained from GaSb.

II. EXPERIMENTAL DETAILS

The samples used in the experiments were diodes of GaAs and GaSb, an undoped GaAs single crystal, and crystals of undoped, Zn-doped, and Te-doped GaSb.

The GaAs diodes were purchasable types (General Electric SSL-4), which were soldered on a copper cold finger after the casing was removed. The GaSb diodes were fabricated by alloying Pb-Se pellets (98% Pb, 2% Se) in[23] p-type GaSb ($N_A - N_D \approx 2\times10^{17}$ cm^{-3}) and were also mounted on a copper cold finger. With current pulses of about 10^4–10^5 A cm^{-2} a minority carrier density in the order of 10^{17} cm^{-3} was generated in both materials.

The epitaxial-grown GaAs crystal ($p = 2\times10^{14}$ cm^{-3}) was excited by a $GaAs_xP_{1-x}$ injection laser about 65 meV above the band gap. The GaSb samples were (i) not intentionally doped-solution-grown crystals, and (ii) Zn-doped boat-grown crystals in a doping range $2.5\times10^{16} \leq N_A - N_D \leq 8.5\times10^{19}$ cm^{-3}, and (iii) Te-doped crystals in a range $0 \lesssim N_D - N_A \leq 1.2\times10^{18}$ cm^{-3}.

The GaSb crystals were immersed in liquid He or were mounted on a crystal holder, which was cooled to 77 or 300 K. They were excited by a Q-switched Nd-YAlG laser, focused on the sample to a peak power density of about 100 kW cm^{-2}. For excitation dependent measurements the intensity of the light could be varied by neutral density filters. A maximum minority carrier density of about 10^{17} cm^{-3} at the crystal surface was estimated. All samples were freshly etched before the measurements.

In all cases, the excitation was carried out pulsewise with about 0.5-μsec pulse duration and a typical repetition rate of 2 kHz. The luminescence was dispersed by a 0.85-m Spex grating double spectrometer or by a 0.25-m Jarrell Ash grating spectrometer. For measurements on GaAs an additional Zeiss double-prism monochromator was used. The luminescence radiation was detected with a RCA 6217 photomultiplier with S-10 response in the case of GaAs and by a RCA C31034 A type with GaAs cathode or a RCA C31000 F with extended red multialkali cathode in the case of GaSb. For additional measurements in the near-band-edge region of GaSb a PbS cell (Santa Barbara Research Center) in connection with conventional lock-in technique was used.

The measurements above the band gap were carried out using a "digital-boxcar-integration" method: The signal was taken as a pulse sequence from the photomultiplier. During the excitation the signal pulses were counted in one counter. Between the excitation pulses the dark count rate was recorded by a second counter. The exact agreement of the count time of both counters was reached by digital setting of the gate times from the same clock. The luminescence spectra were measured stepwise in an automatic cycle with several runs over the whole spectral region. All spectra were corrected for the spectral response of the system, for reabsorption in the sample and for the transfer from the wavelength scale to the energy scale.

III. GaAs–SPECTRA

Figure 2 shows the spectrum of a GaAs diode, which was operated in forward direction. Besides the familiar electroluminescence at $h\nu \approx 1.5$ eV a new emission band appears at $h\nu \approx 1.86$ eV, which is at the used injection current about nine orders of magnitude weaker than the near-band-edge emission. The result obtained from an optical excited pure GaAs crystal is depicted in Fig. 3. Under both excitation conditions, a weak emission band at $h\nu \approx 1.86$ eV is observed. For orientation, the band-structure data[21,22] of GaAs for $E_g + \Delta_0 = 1.86$ eV are drawn in Fig. 3 using $E_g = 1.519$ eV and $\Delta_0 = 0.341$ eV. We suggest

that the new emission band at $h\nu \simeq 1.86$ eV in GaAs is caused by the recombination of free or shallow bound conduction-band electrons with holes in the split-off valence band which are generated by Auger recombination.

Other explanations can be excluded: (i) First, the emission from a band other than the split-off valence band is ruled out: From energetical considerations the recombination of electrons at the X point of the Brillouin zone[24] ($X_{6c} - \Gamma_{6c} \approx 0.38$ eV) with holes at the Γ point must be taken into account. This explanation is improbable, because for the excitation process as well as for the recombination process a momentum transfer over the whole Brillouin zone would be necessary. (ii) Another excitation process of holes into the split-off valence band than excitation by Auger recombination is also excluded. A two-step excitation, which is possible when optical excitation is used, is ruled out by the diode measurement.

To support our interpretation, the order of magnitude of the Auger coefficient C_p(GaAs) for the hhe process including the split-off valence band is estimated from the spectroscopic data. The integrated intensity of the E_g luminescence is given by

$$I_B = FB_{d1} npV_1 , \tag{1}$$

where B_{d1} is the transition coefficient for radiative recombination and V_1 is the radiant volume. The equipment properties are summarized in the factor F. The total intensity of the Auger band is analogously given by

$$I_A = FB_{d2} np_s V_2 = FB_{d2} C_p n^2 p^2 t_s V_2 , \tag{2}$$

where p_s and t_s are the density and the lifetime of the Auger holes in the split-off valence band. The Auger coefficient C_p follows from the ratio I_B/I_A according to Eqs. (1) and (2). The transition coefficients for radiative recombination B_{d1} and B_{d2} are supposed to be nearly equal for both transitions. The ratio of the radiant volumes V_1 and V_2 reduces to the ratio of the reabsorption lengths[25] L_1 and L_2 for the corresponding photon energies: $V_1/V_2 \approx L_1/L_2 \approx (5 \times 10^{-2}\ \text{cm})/(4 \times 10^{-5}\ \text{cm})$. For L_1 the geometrical diode length is set. If one assumes a reasonable carrier density of $n \approx p = (2\text{–}5) \times 10^{17}\ \text{cm}^{-3}$ and a value for the hole lifetime $t_s = 10^{-10}\text{–}10^{-11}$ sec, which has been estimated from a line-shape analysis of the Auger band in GaSb,[11] a value for C_p(GaAs) can be estimated with the experimental intensity ratio $I_B/I_A \approx 10^9$: $C_p(\text{GaAs})_{77\,\text{K}} \approx 10^{-(31\pm1)}\ \text{cm}^6\,\text{sec}^{-1}$.

This value for the Auger coefficient has the same order of magnitude as can be estimated from other measurements or calculations: From the decrease of the quantum efficiency in p-type GaAs at high acceptor concentrations[7] a value of

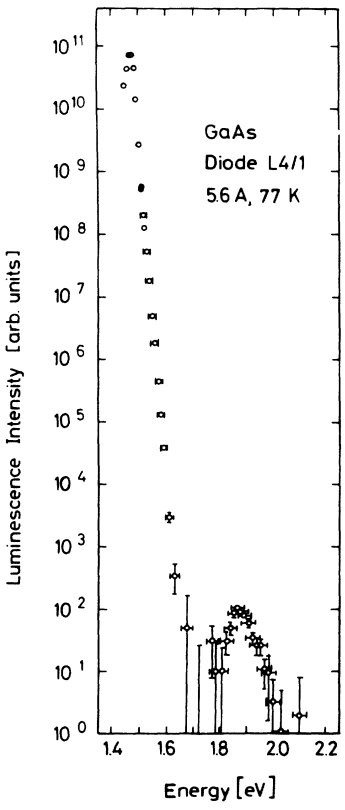

FIG. 2. Electroluminescence of GaAs between 1.4 and 2.2 eV (experimental points with error bars).

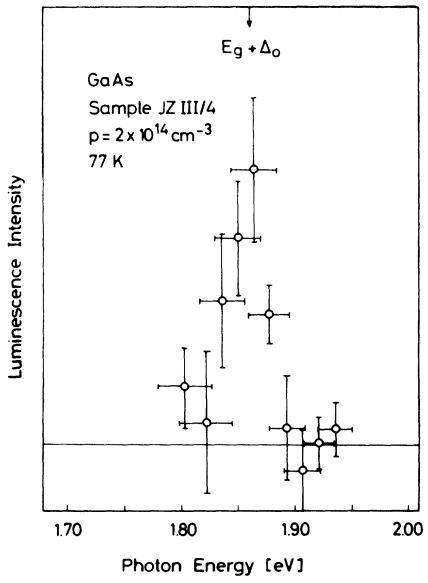

FIG. 3. Photoluminescence of GaAs at 1.86 eV. The arrow indicates the energy data for $E_g + \Delta_0$ (Refs. 21 and 22).

$C_p(\mathrm{GaAs})_{77\,\mathrm{K}} \approx 5 \times 10^{-30}$ cm^6 sec^{-1} can be estimated.[26,27] From the computation of Takeshima[16] a smaller value [$C_p(\mathrm{GaAs})_{300\,\mathrm{K}} \approx 10^{-33}$ cm^6 sec^{-1}] can be deduced, which is predicted to depend strongly on temperature. All methods of estimation lead to the corresponding conclusion that for hole concentrations $p < 10^{19}$ cm^{-3} the hhe Auger recombination in GaAs has no essential influence on the quantum efficiency of the luminescence.

GaAs is a noncentrosymmetric crystal. Therefore, frequency doubling of the E_g luminescence by nonlinear optics is allowed. Figure 4 shows the luminescence spectrum up to $h\nu = 3$eV of the same GaAs diode, operated at an identical injection current as for the spectrum in Fig. 2. The intensity of the second harmonic of the E_g luminescence $h\nu(2\omega) \approx 2.95$ eV has a similar order of magnitude as the Auger band at $h\nu \approx 1.86$ eV. At the injection current used (5.6 A) photon emission between these energies could not be detected even with a measuring time of about one day per point.

In Fig. 5 the dependence of the emission spectra in GaAs at $h\nu \approx E_g + \Delta_0$ on the injection current is shown. The integrated intensity of the Auger band I_A has a superlinear dependence on the injection current i over the whole excitation range ($I_A \propto i^{1.5}$). (Note, that the logarithmic plot pretends a saturation behavior of the emission at $h\nu \approx 1.86$ eV, which is not really the case.)

At the highest injection current of 34 A an emission tail suddenly appears above the Auger band. As Fig. 6 depicts, this luminescence continuum extends up to the second harmonic of the near-band-edge emission. At injection currents greater than 8 A stimulated emission from the GaAs diode takes place. Therefore, the second-harmonic line at $h\nu \approx 2.95$ eV is a relatively strong emission. Above $h\nu = 3$ eV no photon signal could be detected.

It has been confirmed by additional measurements on other GaAs diodes that the luminescence continuum is not observed until a certain threshold current is reached. This threshold is not correlated with the onset of stimulated emission processes. The continuum shows no pronounced structure within the rough experimental resolution. As can be seen from Fig. 5, the intensities of the luminescence continuum and of the Auger band at $h\nu \approx 1.86$ eV are not correlated.

We propose that the luminescence continuum between the onefold and the twofold band-gap ener-

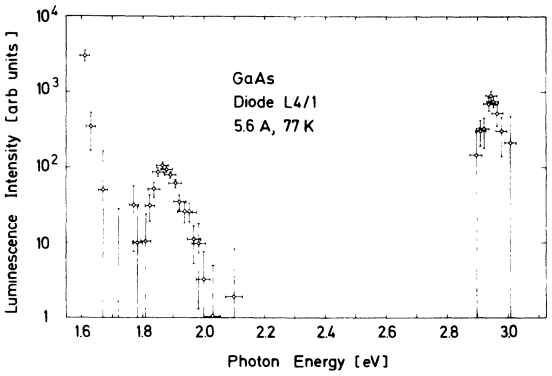

FIG. 4. Electroluminescence of GaAs between 1.6 and 3 eV at equal injection current as for the spectra in Fig. 2.

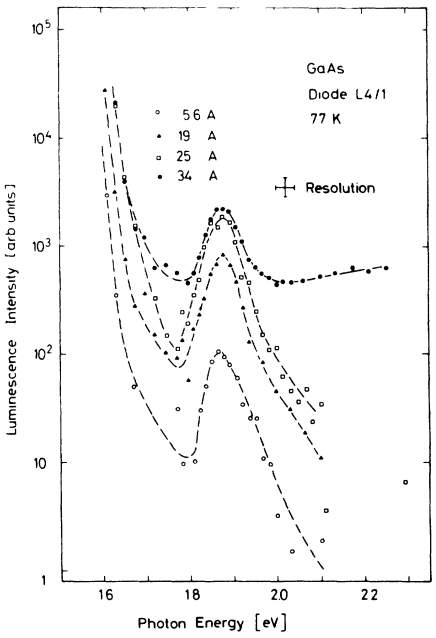

FIG. 5. Luminescence band at $h\nu \approx E_g + \Delta_0$ in GaAs for increasing injection currents.

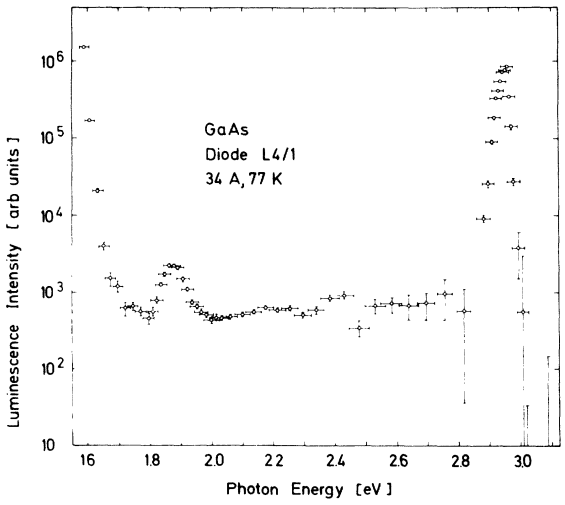

FIG. 6. High-energy luminescence from GaAs at the greatest injection current of 34 A.

gy is caused by the radiative recombination of free or bound holes with Auger electrons which relax to the conduction band minimum. The activation energy for a momentum conserving eeh Auger process could be brought up by a bandfilling mechanism due to the high carrier concentration. As Zschauer[28] pointed out in the example of p-type GaAs, the Auger transition rate will increase rapidly when the bandfilling exceeds a certain threshold. The threshold energy for band-to-band Auger recombination in n-type GaAs is not accurately known.[17] Nevertheless, an electron concentration of about 10^{18} cm^{-3} should be a reasonable value.

The required activation energy E_a could be determined from the high-energetic edge of the luminescence continuum. The luminescence tail should extend up to $h\nu = 2E_g + E_a$, if the radiative recombination is without phonon participation, or up to $h\nu = 2E_g + E_a - \hbar\omega$, if the radiative recombination of the Auger electrons is phonon accompanied. Since the high-energetic side of the continuum is covered by the frequency doubled of the E_g band, the break of the continuum cannot be determined. Therefore, it cannot be decided if the threshold behavior of the emission continuum is caused by a momentum conserving Auger process. Furthermore, the hhe Auger process shows no threshold behavior under our experimental conditions, in spite of the fact that it should occur as well.[28]

On the other side, the threshold character of the continuum could be caused by the special experimental conditions: It seems to be possible that only at very high injection currents an appreciable injection of holes into the n side of the pn junction takes place, where the eeh process should mainly occur. A comparison with other experimental results speaks in favor of this possibility: The experimental energy-distribution curve of the Auger electrons, emitted from a cesium-coated GaAs surface, published by Pancove *et al.*,[8] reveals no activation energy for the eeh Auger recombination. (On the contrary, these measurements indicate an energy deficit compared with $2E_g$. Therefore, it can be presumed that the eeh Auger process in GaAs is phonon participated.[3])

IV. GaSb–SPECTRA

Electroluminescence spectra around $h\nu \approx 2E_g$ of a GaSb diode at two different injection currents are shown in Figs. 7 and 8. Figure 9 depicts a typical photoluminescence spectrum of an undoped GaSb crystal at 4.2 K under Nd-YAlG laser excitation in the same spectral region. For orientation the energy data of the GaSb band structure

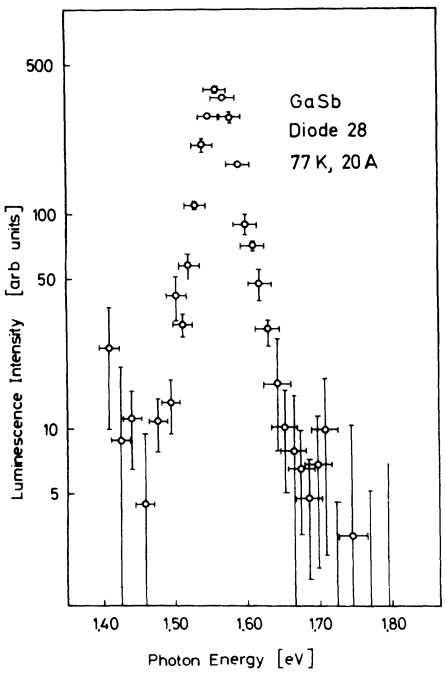

FIG. 7. Electroluminescence of GaSb between 1.40 and 1.80 eV. Injection current 20 A.

for $E_g + \Delta_0$ and $2E_g$ are included in this figure[14,15] ($E_g = 0.812$ eV; $\Delta_0 = 0.749$ eV). (Note that Figs. 7 and 8 are semilogarithmic plots, whereas Fig. 9 is a linear plot.)

As in the case of GaAs, a broad emission band

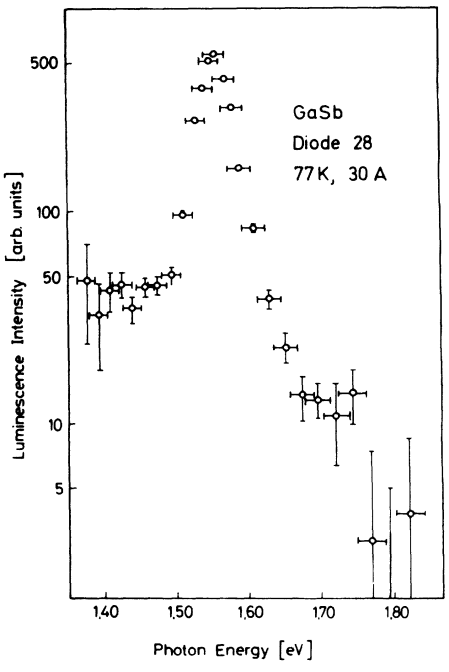

FIG. 8. Electroluminescence of GaSb between 1.40 and 1.80 eV. Injection current 30 A.

(halfwidth 50 meV) is detected in GaSb at a photon energy of $E_g + \Delta_0$. Further, energetically below $h\nu \approx 2E_g$ a weak continuum appears in the spectra. The emission continuum, which is unstructured within the rough experimental resolution, is observed in a photon energy range of 1.50–1.05 eV (see Fig. 10). At still lower photon energies the emission continuum passes into the Boltzmann tail of the emission band at E_g.

Both emission processes in GaSb above the band gap, the luminescence band at $h\nu = E_g + \Delta_0$ and the continuum at $h\nu \lesssim 2E_g$, are ascribed to the radiative recombination of Auger carriers. A two-step excitation mechanism, which is the only possible alternative explanation, can be excluded for both emissions. In the case of a two-step excitation by the laser light, the luminescence continuum should extend from $h\nu = E_g$ to $h\nu = E_g +$ laser energy, which is not found experimentally. (The excitation of electrons by the reabsorption of across-the-gap radiative recombination is still more improbable since the internal quantum efficiency is much smaller than 1.) For the emission band at $h\nu = E_g + \Delta_0$ a two-step mechanism is excluded from intensity arguments: In the case of a two-step excitation, the ratio of the second harmonic of the primary light and the $E_g + \Delta_0$ emission should have the same order of magnitude for both investigated materials, GaAs and GaSb.[29] In the case of GaAs a relatively strong frequency doubled emission of the E_g light compared with the Auger band has been recorded (compare Fig. 4); whereas in the case of GaSb the second harmonic of the E_g emission is covered by the emission band at $h\nu = E_g + \Delta_0$ (see Fig. 9).

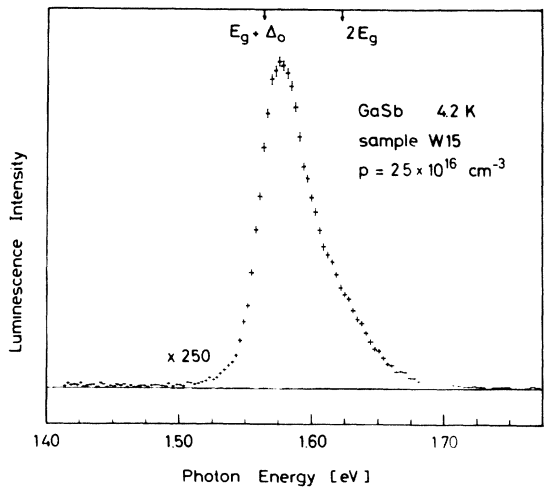

FIG. 9. Photoluminescence of undoped GaSb above the band gap at 4.2 K. The arrows indicate the energy data for $E_g + \Delta_0$ and $2E_g$ (Refs. 14 and 15). The intensity scale is the same as for Figs. 11 and 12.

The integrated intensity of this band is even several orders of magnitude stronger than the frequency doubled laser light.[30] For this reasons a two-step mechanism can be excluded.

The emission band at $h\nu \approx 1.57$ eV in undoped GaSb is interpreted as the radiative recombination of conduction-band electrons with holes in the split-off valence band which are excited by a hhe Auger mechanism. As can be gathered from the error bars of the experimental points in Fig. 9, the absolute intensity of the Auger band in GaSb is much higher than that in GaAs. The experimental data indicate that the hhe Auger recombination creating holes in the split-off valence band has a greater transition probability in GaSb than in GaAs. This fact verifies our assumption, that GaSb is a good model for studying the Auger recombination.

The weak luminescence continuum at photon energies between 1.05 and 1.50 eV is ascribed to the radiative recombination of relaxing Auger particles. Similar to the results on GaAs diodes, the intensity of the continuum for GaSb diodes is not correlated with that of the Auger band: When the injection current of the investigated GaSb diode 28 is increased from 20 to 30 A (see Figs. 7 and 8), the intensity of the continuum increases by a factor of 5 whereas the Auger band grows only by a factor of about 1.5. Therefore, as in the case of GaAs, the luminescence continuum is proposed to be caused by the radiative recombination of relaxing Auger electrons in the conduction band with thermalized holes.

Photoluminescence measurements on doped GaSb crystals confirm this explanation. Figures 11 and 12 show the results obtained from higher doped p-type and n-type samples, respectively. The spectra in the Figs. 9, 11, and 12 are given on the same (linear) intensity scale. (Note the

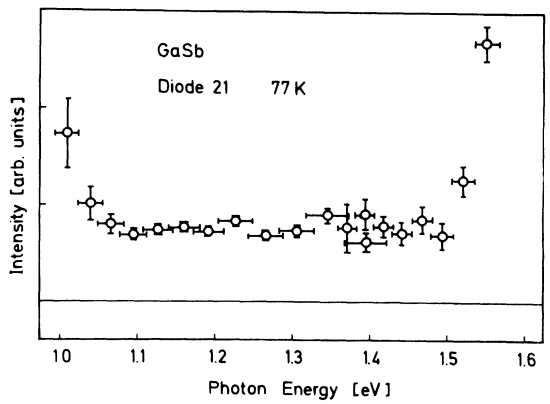

FIG. 10. Electroluminescence of GaSb between 1.0 and 1.55 eV. (Linear plot; note, that another diode was used than for Figs. 7 and 8.)

respective multiplication factors which are necessary to show the peak heights in the same magnitude.) No correlation between the intensities of the emission tail and of the Auger band is found.

As is expected for a band-to-band transition, the Auger band broadens at higher doping levels and the peak position shows an energy shift. Figure 13 is a systematic plot of the peak position of the Auger band at different doping levels, measured at 4.2 and 77 K. The blue shift in n-type samples is ascribed to a bandfilling mechanism (Burstein-Moss shift). The red shift is explained by tail states or an acceptor band at the split-off valence band.

A very surprising effect is the great intensity of the Auger band in n-type GaSb. In degenerate n-type material it is even possible to use conventional lock-in technique for recording a spectrum above the band gap. The Auger emission is much stronger than in doped p-type samples, where the hhe Auger mechanism creating holes in the split-off valence band should be more probable. Instead of such an efficient hhe Auger recombination the eeh process should occur in n-type GaSb due to the high electron density. This recombination, however, would not lead to the observed emission band at $h\nu \approx 1.6$ eV, but to the already discussed luminescence continuum from about the twofold to the onefold energy gap. Experimentally, the continuum for n-type GaSb is only by a factor of 50 stronger than for p-type material. We explain

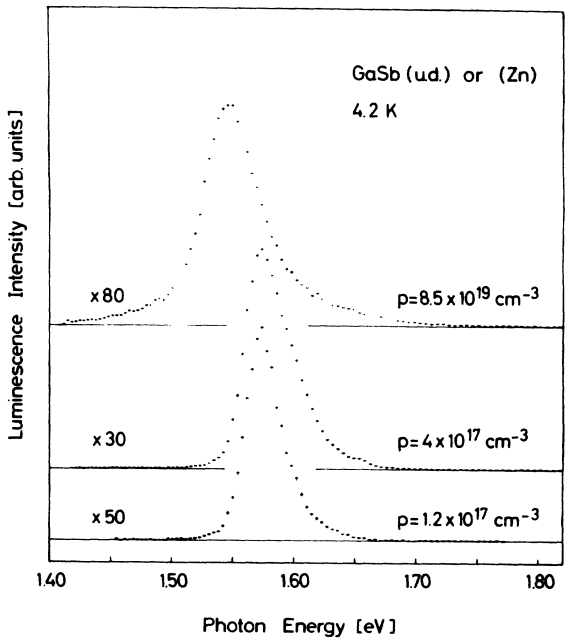

FIG. 11. Auger band in undoped (ud) and Zn-doped p-type GaSb at 4.2 K (uniform intensity scale).

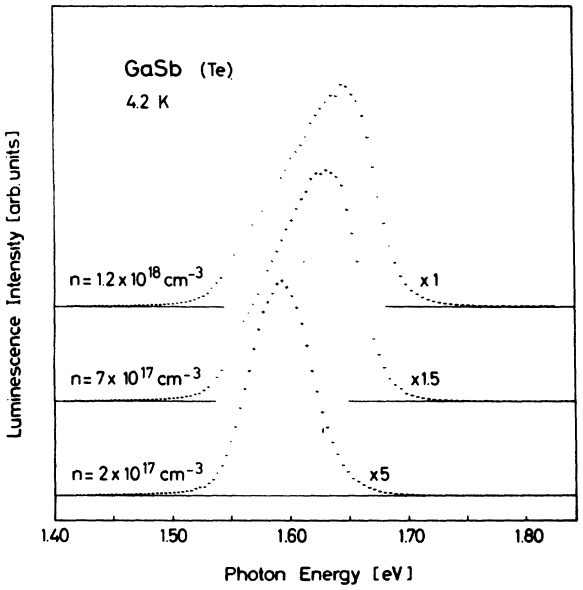

FIG. 12. Auger band in Te-doped n-type GaSb at 4.2 K (uniform intensity scale).

the higher intensity of the Auger band in n-type GaSb by an Auger mechanism including bound holes. This will be stated in more detail in Sec. V.

V. REACTION KINETICS OF AUGER PROCESSES IN GaSb

In the following, the reaction kinetics of the Auger band in GaSb is studied and its characteristic feature is compared with the near-band-edge emission. The varied parameters are laser ex-

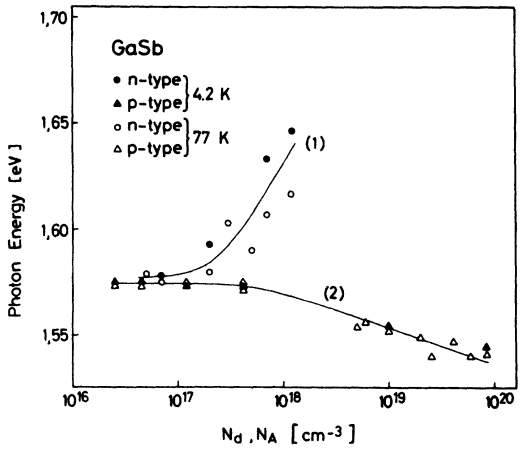

FIG. 13. Dependence of the energetical peak position of the Auger band on the doping concentration (dopants: Zn and Te). Experimental values are given for 77 and 4.2 K, without correction for the temperature dependence of $E_g + \Delta_0$.

citation power and sample doping level.

Under steady-state conditions, the variation of the minority carrier density is given by

$$\frac{dn}{dt} = \frac{dp}{dt} = G - R = 0 , \tag{3}$$

with

$$R = A_n n + A_p p + Bnp + C_n n^2 p + C_p p^2 n \quad (+ C_p' N_A pn) ,$$

where G and R are generation and recombination rate. The diffusion term is neglected in Eq. (3) because the laser penetration depth is of the same order of magnitude as the diffusion length (some μm). The total recombination rate R considers band-to-trap recombination (process I) with recombination coefficients A_n and A_p for electron and hole capture, respectively; radiative band-to-band recombination (process II) with recombination coefficient B; and Auger recombination (band-band and band-acceptor processes, process III and process II′, with recombination coefficients C_n, C_p, and C_p'). The marking of the recombination processes with roman ciphers simultaneously reproduces the order of the corresponding process relative to the free carriers. Different terms of recombination in Eq. (3) may be expected to dominate at different carrier concentrations. Table I shows the dependence of the minority carrier density on the generation rate G in the intrinsic and in the extrinsic case (example p-type material).

As Table I illustrates, in the intrinsic case the dominating recombination process can be deduced from an analysis of the excitation dependence of the minority carrier density ($n_{\mathrm{I}} \propto G, n_{\mathrm{II}} \propto G^{1/2}$, $n_{\mathrm{III}} \propto G^{1/3}$). Under extrinsic conditions, the carrier density is always proportional to the generation rate.

A. Experiments on p-type GaSb

The Figs. 14 and 15 show the experimental dependence of the luminescence intensities at E_g and at $E_g + \Delta_0$ on the laser excitation power for a Zn-doped sample and for an undoped sample, respectively. For illustration an E_g spectrum (band-to-band recombination) and a spectrum of the Auger band, both at the highest excitation density of about 100 kW cm^{-2}, are given in Figs. 14(b) and 14(c). Since the line shapes of the emission bands show no variation at lower excitation densities, only peak intensities are drawn in Fig. 14 and in Fig. 15. Both measurements show a quadratic connection between the intensity of the Auger

TABLE I. Dependence of the minority carrier density on the generation rate G in the intrinsic case and in the extrinsic case (example p-type material).

Dominating recombination process	Intrinsic conditions	Extrinsic conditions
I	$n, p \propto G/A$	$n \propto G/A$
II	$n, p \propto (G/B)^{1/2}$	$n \propto G/Bp$
II′	$n, p \propto (G/C'N_A)^{1/2}$	$n \propto G/C'N_A p$
III	$n, p \propto (G/C)^{1/3}$	$n \propto G/Cp^2$

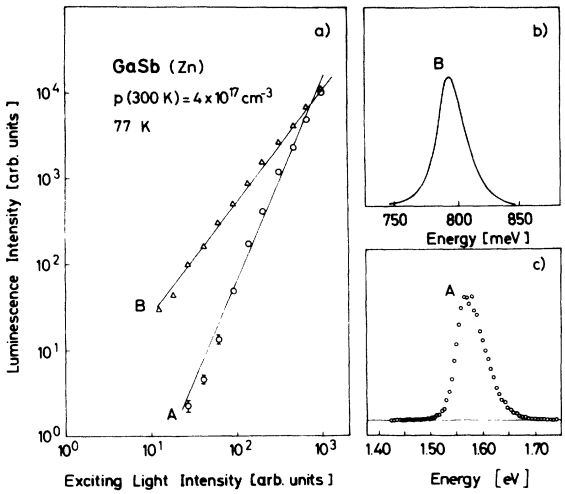

FIG. 14. Dependence of the E_g and $E_g + \Delta_0$ emission intensities on the exciting laser power in Zn-doped GaSb (part a). For illustration, the E_g spectra (B) and the Auger band (A) at the highest excitation intensity of 100 kW cm^{-2} are shown (part b and c).

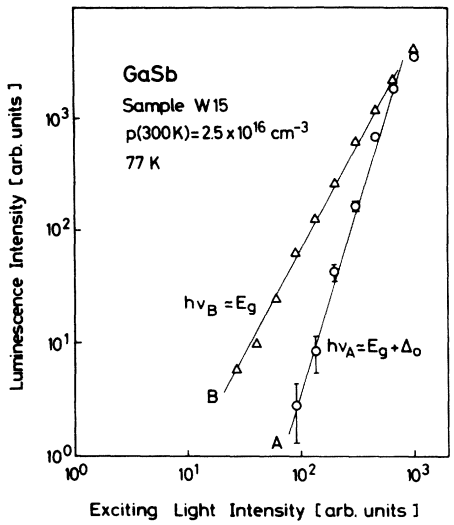

FIG. 15. Dependence of the near-band-edge (B) and of the Auger recombination involved emission (A) on exciting laser power (peak intensities). The highest laser density was 100 kW cm^{-2}.

band I_A (circles) and that of the band-to-band emission I_B at E_g (triangles): $I_A \propto I_B^2$. This dependence is expected because the E_g luminescence is proportional to np and the Auger band is proportional to n^2p^2. For the undoped sample in Fig. 15 (intrinsic condition) a satisfactory agreement with the experimental excitation dependence is obtained, when the carrier density $n=p$ is supposed to be proportional to the generation rate G (compare Table I, intrinsic condition case I). Then the expected excitation dependencies $I_B \propto np \propto G^2$ and $I_A \propto n^2p^2 \propto G^4$ are in accordance with the experimental exponents 1.8 for line B and 3.4 for line A. The measurement on the Zn-doped sample (extrinsic condition) yields an experimental dependence of $I_B \propto G^{1.2}$ and $I_A \propto G^{2.4}$, which is in good agreement with the expected linear and quadratic dependence. Luminescence studies on p-type GaSb at various doping levels are presented in Fig. 16 [(a) measurements at 77 K; (b) measurements at 300 K]. Freshly etched samples were investigated and the integrated emission intensities at E_g (triangles) and at $E_g + \Delta_0$ (circles) under identical experimental conditions are shown. Naturally, the measured points are strongly scattered. Nevertheless, the full lines reflect the systematic feature of the experimental values: As is expected, the connection $I_G \propto I_B^2$ is valid in good approximation.

According to Table I, the doping dependence of the luminescence intensities I_A and I_B are given[31] by

$$
\begin{aligned}
&I_B \propto np, \\
&I_B \propto (G/A)p \propto p \quad \text{if recombination process I dominates,} \\
&\left.\begin{aligned} I_B &\propto (G/Bp)p \\ I_B &\propto (G/C'N_A p)p \end{aligned}\right\} \text{const if process II or II' dominates,} \\
&I_B \propto (G/Cp^2)p \propto p^{-1} \quad \text{if process III dominates.}
\end{aligned} \tag{4}
$$

And analogously

$$
\begin{aligned}
&I_A \propto n^2p^2, \\
&I_A \propto p^2 \quad \text{for part I,} \\
&I_A \propto \text{const} \quad \text{for part II or II',} \\
&I_A \propto p^{-2} \quad \text{for part III.}
\end{aligned}
$$

From the decrease of the emission intensities proportional to p^{-1} and p^{-2} for the E_g luminescence and the Auger band, respectively [compare Fig. 16 and relation (4)], it is concluded that band-to-band Auger recombination is the charge-carrier lifetime dominating process at high carrier densities. For comparison, the quantum efficiency curves of Queisser and Panish[7] on GaAs are included in Fig. 16 (dashed lines). Seemingly independent on the different band-structure data, the decrease of the luminescence efficiency takes place at about the same hole concentration in both materials. For GaSb, however, in part II of the efficiency curve an internal quantum efficiency $\eta_i \ll 1$ is estimated. Therefore, it is concluded that the horizontal part II in Fig. 16(a) is not caused by radiative recombination, but by nonradiative recombination of second order. A possible nonradiative recombination of second order is a band-acceptor Auger recombination (compare process II' in Table I).

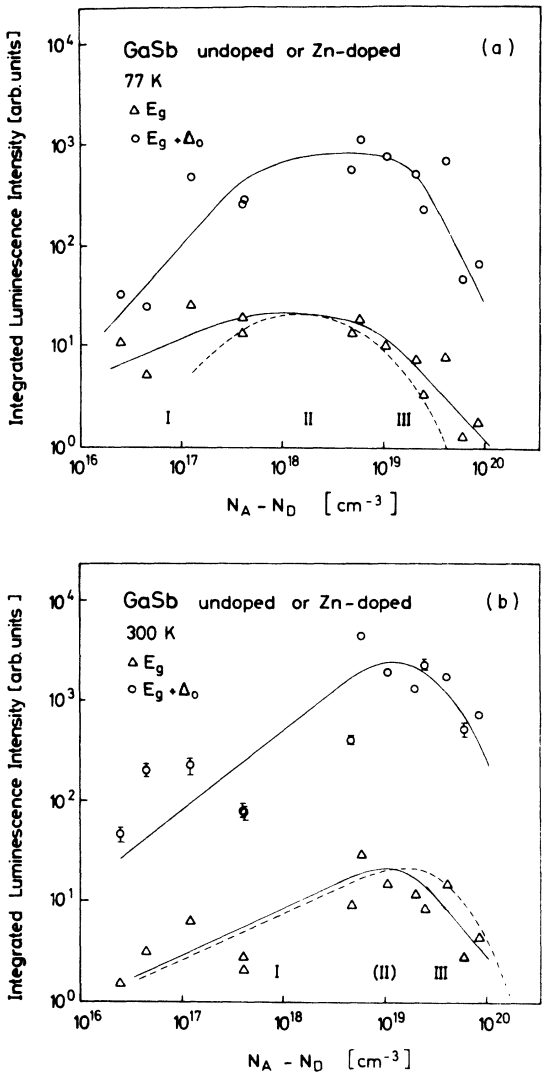

FIG. 16. Dependence of the luminescence efficiency for the E_g and the $E_g + \Delta_0$ emission bands on the acceptor concentration $N_A - N_D$. (a) Obtained at 77 K; (b) at 300 K. The constant laser density was 100 kW cm^{-2}. The solid lines are for clarification of the experimental dependence. The broken lines represent similar experiments on p-type GaAs (Ref. 7).

B. Experiments on n-type GaSb

Figure 17 is a plot of the total emission intensity of the E_g luminescence (triangles) and of the Auger band (circles) as a function of the Te-doping concentration, measured at 77 K. The intensities in this diagram are given on the same intensity scale as for Fig. 16. In Fig. 17 the intensity of the Auger band increases strongly with growing Te concentration. At high Te doping it is considerably stronger than in p-type material. The total intensity of the E_g emission (integrated over all emission lines) remains constant.

The emission intensities of the observed luminescence bands as a function of the laser excitation power are shown in Fig. 18 for a n-conducting sample ($N_D > N_A$) and in Fig. 19 for a compensated sample with $N_D \approx N_A$. The near-band-edge emission spectra shows two broad bands at high excitation conditions [see Fig. 18(b)]. Line B is an (e, h) transition (including tail states and shallow acceptors). Line C is ascribed to a (e, A^-) transition.[32,33] The acceptor A, which is always present in GaSb, is caused by a native lattice defect[18,19] ($V_{GA} + Ga_{Sb}$) and has hole binding energies of 34.5 and 102 meV.[34]

In contrast to p-type GaSb, the Auger recombination involved emission in n-type GaSb does not show the $I_A \propto I_B^2$ law. On the basis of a band-acceptor Auger recombination a reasonable explanation of the intensity, the doping dependence and the excitation dependence of the Auger band in n-type GaSb is possible. As can be deduced from the strong C line, which shows no saturation at higher excitation, the native acceptor has a high concentration. Since this acceptor can bind two localized holes, the recombination of one hole with a conduction-band electron has a large Auger probability.[20] Thereby the second hole is pushed into the split-off valence band. A bandfilling of about 70 meV will lead to a resonant impact process because the recombination energy, which is transferred to the second hole, corresponds to the

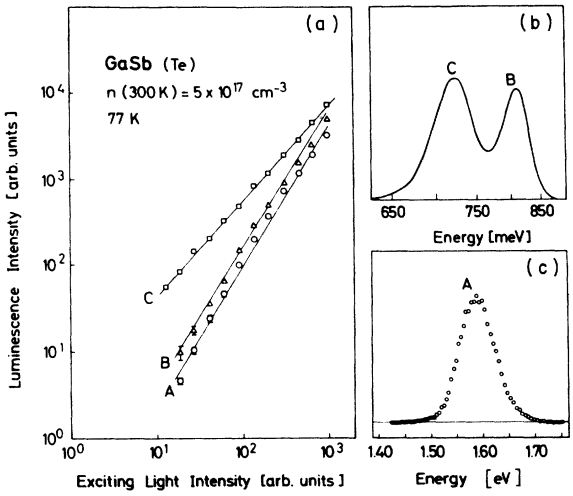

FIG. 18. Dependence of the E_g and $E_g + \Delta_0$ emission intensities on the exciting laser power in n-type GaSb(Te) (part a). The E_g spectra and the $E_g + \Delta_0$ spectra—both at the highest laser light density of 100 kW cm^{-2}—are shown in parts b and c.

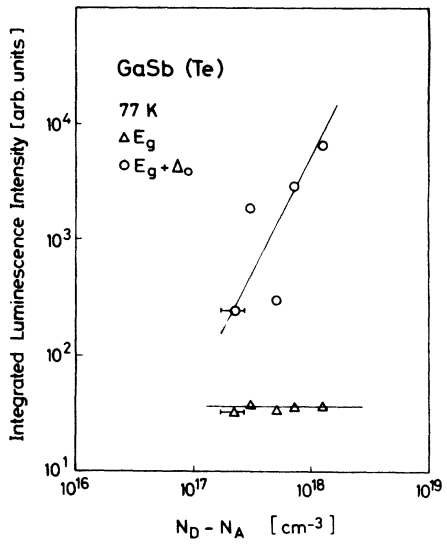

FIG. 17. Luminescence efficiency in n GaSb at 77 K. The constant exciting light density was 100 kW cm^{-2}.

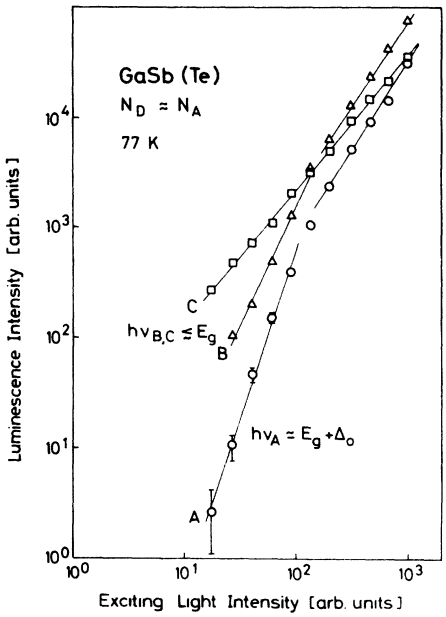

FIG. 19. Excitation power dependences measurement on compensated GaSb(Te) with $N_D \approx N_A$.

energetic difference to the split-off valence band. In n-type GaSb, the native acceptor acts as (A^{--}) center in equilibrium. Nevertheless, under high excitation conditions the acceptor will bind two holes in zones near the crystal surface[35] where the Auger signal is created.

The relatively strong intensity of the Auger band and its increase with growing tellurium concentration (compare Fig. 17) can be explained by a self-compensation effect. From infrared absorption measurements it is known[36] that the native defect in GaSb increases either under irradiation with electrons or by Te doping.

The excitation dependence of the luminescence bands is explained as follows: For the low Te-doped sample (see Fig. 19) it is presumed that the second ionization state of the deep native acceptor is saturated. Then, under intrinsic conditions and first-order reaction kinetics, the excitation dependences are given according to Table I:

$$\begin{aligned}&(e, A^{-}_{\mathrm{sat}}) \text{ recombination: } I_c \propto N_{A\mathrm{sat}} \times n \propto G^1,\\ &(e, h) \text{ or } (e, A^0) \text{ recombination: } I_B \propto pn \propto G^2, \qquad (5)\\ &(e, h_s) \text{ recombination: } I_A \propto N_{A\mathrm{sat}} \times pn^2 \propto G^3.\end{aligned}$$

The predicted values agree excellently with the experimental dependence in the low excitation range

$$I_{c,\mathrm{exp}} \propto G^{1.1}; \quad I_{B,\mathrm{exp}} \propto G^{2.1}; \quad I_{A,\mathrm{exp}} \propto G^3.$$

At higher excitation, the effect of second-order reaction kinetics must be considered. In consequence of quite different reabsorption factors of the emission lines A, B, and C, the recorded luminescence signals are produced in different crystal depths with a distinct excitation rate.[35] Two borderline cases are easy to survey: For the Auger band A with strong reabsorption the condition $n, p \propto G^{1/2}$ is fulfilled, which yields a theoretical dependence of $I_A \propto G^{1.5}$ at higher excitation (experimental exponent 1.6). Line C ($h\nu_c < E_g$) is created in deeper lying crystal zones where $n, p \propto G$ is still valid.

At higher tellurium concentration (see Fig. 18), the native acceptor is an (A^{--}) center in equilibrium. As is expected, the capture of holes on the second ionization state is proportional to the generation rate: $I_{c,\mathrm{exp}} \propto G^{1.1}$. Since this capture on charged centers should be very effective, for the free and shallow bound holes follows a superlinear density dependence. This explains both, the experimentally identical and superlinear excitation dependence of the A line and B line. The A line is expected to be proportional to the $(A^{--})^{++}$ concentration. The B line includes recombination with free and shallow-bound holes [$I_B \propto p$ and $(A^{--})^{++}$].

VI. TRANSITION COEFFICIENT FOR AUGER RECOMBINATION IN p GaSb

From the decrease of the luminescence intensity in Fig. 16(a) at higher Zn doping, the Auger coefficient for hhe recombination can be estimated. For the break at $p_x \approx 10^{19}$ cm^{-3} of the emission, efficiency curve holds:

$$B_d n p_x (\eta_i)^{-1} = C_p n p_x^2. \qquad (6)$$

Part II of the efficiency curve is formally ascribed to radiative recombination with a transition coefficient B_d and an internal quantum efficiency η_i [left-hand side of Eq. (6)]. Two independent methods of estimate give an internal quantum efficiency $\eta_i = 10^{-(3\pm1)}$ at 77 K. Thereby, the luminescence intensity is compared with the laser signal from the reflecting crystal surface. The other evaluation is carried out in considering the luminescence signal, the sensitivity of the detecting system and correction factors because of reabsorption and reflection in the sample. From Eq. (6) follows for the hhe band-to-band Auger coefficient C_p(GaSb) at 77 K, using a value[27] for $B_d \approx 10^{-9}$ cm^3 sec^{-1}:

$$C_p(\mathrm{GaSb})_{77\ \mathrm{K}} \approx 10^{-(25\pm1)}\ \mathrm{cm}^6\,\mathrm{sec}^{-1}.$$

In the following, the experimental C_p (GaSb) will be compared with theoretical predicted values. According to Beattie and Landsberg,[12] the Auger transition rate is given by an expression of the form

$$W_{\mathrm{Auger}} \propto \sum_{k_1 k_2} \sum_{k_1' k_2'} \left| \frac{1}{(\Delta k_{1,1';2,2'})^2 + \lambda^2} \right|^2 \times \delta(E)\theta(1, 1', 2, 2'),$$

where

$$E = E_1' + E_2' - E_1 - E_2. \qquad (7)$$

The charge carriers with momentum k_i interact via a screened Coulomb potential (reciprocal screening length λ). $\theta(1, 1', 2, 2')$ is a statistic factor which leads to an activation energy E_a for the Auger process,[13] when it is minimized under consideration of energy and momentum conservation and by taking the band structure as a basis. Assuming a parabolic band structure this activation energy for a hhe Auger process involving the split-off valence band is given in the Boltzmann approximation[16]

$$E_a = (E_g - \Delta_0) m_s / (2m_{\mathrm{hh}} + m_e - m_s). \qquad (8)$$

Hence it follows[37] an activation energy $E_a = 12$ meV for GaSb, which can be easily reached thermally. From the calculations of Takeshima,[16] where a Boltzmann distribution is used, an Auger coefficient C_p(GaSb) $\approx 10^{-27}$ cm^6 sec^{-1} is extrapolated at

a temperature of 300 K. Regarding the small activation energy this Auger coefficient should be nearly independent on temperature.

In the Fermi limit the activation energy of the charge carriers is brought up by a bandfilling mechanism, whereby holes in the heavy hole band give the main contribution.

According to Zschauer[28] and Rosenthal,[17] the drop of the charge-carrier lifetime, which is controlled by a hhe Auger recombination, takes place between a bandfilling E_1 and E_2 of the heavy-hole band, with

$$E_1 = (E_g - \Delta_0)(m_s - m_e)[2(2m_{hh} + m_e - m_s)]^{-1} ,$$
$$E_2 = (E_g - \Delta_0)[4(m_{hh}/m_s) - 2]^{-1} . \quad (9)$$

For GaSb follows[37] a bandfilling of $E_1 = 4.5$ meV to $E_2 = 6.5$ meV, which corresponds to a hole density[38] of $p_x = (4-7) \times 10^{17}$ cm^{-3}. From this predicted break of the theoretical quantum efficiency curve (decreasing from $\eta_i \approx 1$) and according to Eq. (6) follows a hhe Auger coefficient C_p $(\mathrm{GaSb})_{77\,\mathrm{K}} \approx 2 \times 10^{-28}$ cm^{6}sec^{-1}. This value is smaller than the experimental determined value $C_p(\mathrm{GaSb})_{77\,\mathrm{K}} \approx 10^{-(25\pm1)}$ cm^6 sec^{-1}. The theoretical estimation, however, is only valid for $T = 0$, momentum conservation for the Auger process and Burstein-Moss filling of the valence band. Not considered are tail states, which reduce the effective band gap, and excited holes. Nevertheless, the agreement between the theoretical values and the experimental coefficient is rather good when the approximations of the theory and the experimental uncertainty is taken into account.

VII. SUMMARY

Luminescence measurements as a method of investigation of the Auger recombination in the III-V compounds GaAs and GaSb have been presented. The Auger particles have been proved by detecting the extremely weak photon signal above the band gap which is created by the radiative recombination of relaxing Auger particles with charge carriers in the opposite band.

In both materials, GaAs and GaSb, under electrical or optical excitation a broad luminescence band at the photon energy $h\nu = E_g + \Delta_0$ is found as an uniform result, where E_g is the respective energy gap and Δ_0 is the respective spin-orbit splitting of the valence band. This confirms the expectation that in both substances, when a hhe Auger process takes place, the transition of the second hole into the split-off valence band has a greater transition probability than transitions of the second hole into the light-hole band or into the heavy-hole band.

The effect of the different band-structure data of GaAs and GaSb on the intensity of the Auger luminescence spectra and especially on the Auger recombination coefficients is discussed. From spectroscopic data an order of magnitude estimation of the Auger coefficients C_p is performed which yields

$$C_p(\mathrm{GaAs})_{77\,\mathrm{K}} \approx 10^{-(31\pm1)}\ \mathrm{cm^6\,sec^{-1}} ,$$
$$C_p(\mathrm{GaSb})_{77\,\mathrm{K}} \approx 10^{-(25\pm1)}\ \mathrm{cm^6\,sec^{-1}} .$$

The stronger Auger luminescence intensities in GaSb and the relatively great value for the hhe Auger coefficient of GaSb reflect the model character of this substance for Auger recombination.

An extremely weak luminescence continuum in both materials between the onefold and the twofold band-gap energy is explained by the radiative recombination of relaxing Auger electrons in the conduction band with thermalized holes. The threshold behavior of the intensity of the continuum in diode measurements could be explained by the special experimental conditions (injection of holes) rather than by a momentum conserving Auger process.

The energy and the line shape of the Auger band in GaSb can be definitely influenced by the sample doping, showing the familiar effects of band-gap shrinkage and Burstein-Moss shift. The reaction kinetics of Auger processes in doped GaSb have been studied and compared with the near band-gap emissions by measurements at varying doping level and different laser excitation power. As is expected, for p-type GaSb the intensity of the Auger band I_A is proportional to I_B^2, where I_B is the near-band-gap emission intensity. In n-type GaSb(Te) a more complicated dependence is found, which is explained by the role of the native defect in GaSb, which forms a twofold ionizable acceptor. It has been concluded that in p-type GaSb band-band Auger recombination and in n-type GaSb band-acceptor Auger processes lead to the luminescence band at $h\nu = E_g + \Delta_0$.

ACKNOWLEDGMENTS

The authors wish to thank Professor M. H. Pilkuhn for supporting the experiments, and W. Jakowetz and K. H. Zschauer for providing GaSb and GaAs crystal material.

†Work supported by the Deutsche Forschungsgemeinschaft.

*Present address: Robert Bosch GmbH, Abt. FNF D-7000 Stuttgart-30.

[1]P. T. Landsberg, Phys. Status Solidi 41, 457 (1970).
[2]A. Haug, in *Festkörperprobleme XII Advances in Solid State Physics*, edited by O. Madelung (Pergamon, Braunschweig, 1972), p. 411.
[3]R. Conradt, in *Festkörperprobleme XII Advances in Solid State Physics*, edited by O. Madelung (Pergamon, Braunschweig, 1972), p. 449.
[4]P. T. Landsberg and M. J. Adams, J. Lumin. 7, 3 (1973).
[5]J. Krausse, Solid-State Electron. 17, 427 (1974).
[6]T. S. Moss, Proc. Phys. Soc. Lond. B 66, 993 (1953).
[7]H. J. Queisser and M. B. Panish, J. Phys. Chem. Solids 28, 1177 (1967).
[8]J. I. Pancove, L. Tomasetta, and B. F. Williams, Phys. Rev. Lett. 27, 29 (1971).
[9]R. Conradt and W. Waidelich, Phys. Rev. Lett. 20, 8 (1968); R. Conradt, Z. Phys. 209, 445 (1968).
[10]K. Betzler, Solid State Commun. 15, 1837 (1974).
[11]G. Benz and R. Conradt, in *Proceedings of the 12th International Conference on the Physics of Semiconductors, Stuttgart*, 1974, edited by M. Pilkuhn (Teubner, Stuttgart, 1974), p. 1262.
[12]A. R. Beattie and P. T. Landsberg, Proc. R. Soc. A 249, 16 (1958).
[13]P. T. Landsberg, Solid State Commun. 10, 479 (1972).
[14]A. Baldereschi, N. O. Lipari, Phys. Rev. B 3, 439 (1971).
[15]M. Reine, R. L. Aggarwal, and B. Lax, Solid State Commun. 8, 35 (1970).
[16]M. Takeshima, J. Appl. Phys. 43, 4114 (1972).
[17]W. Rosenthal, Solid State Commun. 13, 1215 (1973).
[18]Y. J. van der Meulen, J. Phys. Chem. Solids 28, 25 (1967).
[19]J. Allegre, M. Averons, and G. Bougnot, Cryst. Lattice Defects 1, 343 (1970).
[20]M. K. Sheinkman, Fiz. Tverd. Tela 5, 2780 (1963) [Sov. Phys.-Solid State 5, 2035 (1964)].
[21]D. D. Sell, R. Dingle, S. E. Stokowski, and J. V. Di Lorenzo, Phys. Rev. Lett. 27, 1644 (1971); D. D. Sell, S. E. Stokowski, R. Dingle, and J. V. Di Lorenzo, Phys. Rev. B 7, 4568 (1973).
[22]M. Reine, R. L. Aggarwal, and B. Lax, and C. M. Wolfe, Phys. Rev. B 2, 458 (1970).
[23]A. R. Calawa, J. Appl. Phys. 34, 1660 (1963).
[24]G. D. Pitt and J. Lees, Solid State Commun. 8, 491 (1970).
[25]M. Sturge, Phys. Rev. 127, 768 (1962).
[26]Under identical considerations that will be done in Sec. VI this value for C_p (GaAs) follows from Eq. (6) with $B_d = 3 \times 10^{-8}$ cm^3 sec^{-1} (Ref. 27) and the assumption that $\eta_i \approx 1$ in the case of GaAs. For the break of the experimental quantum efficiency curve at 77 K an acceptor concentration $p_x \approx 6 \times 10^{18}$ cm^{-3} is supposed [Ref. 7, also compare Fig. 16(a)].
[27]Y. P. Varshni, Phys. Status Solidi 19, 459 (1967); 20, 9 (1967).
[28]K. H. Zschauer, Solid State Commun. 7, 1709 (1969).
[29]J. J. Wynne and N. Bloembergen, Phys. Rev. 188, 1211 (1969).
[30]G. Benz and R. Conradt, Phys. Rev. Lett. 34, 1551 (1975).
[31]Only the extrinsic condition is considered. The intrinsic condition results in the identical doping dependence for parts I, II, and II' of Table I. Part III is not realistic in the intrinsic case.
[32]A. A. Kastal'skii, T. Risbaev, I. M. Fishman, and Yu. G. Shreter, Sov. Phys.-Semicond. 5, 1391 (1972).
[33]W. Rühle, W. Jakowetz, and M. H. Pilhuhn in *Luminescence of Crystals, Molecules and Solutions*, edited by F. Williams (Plenum, New York, 1973), p. 444.
[34]W. Jakowetz, W. Rühle, K. Breuninger, and M. H. Pilkuhn, Phys. Status Solidi A 12, 169 (1972).
[35]G. Benz and R. Conradt, J. Lumin. 12/13, 551 (1976).
[36]R. Kaiser and H. Y. Fan, Phys. Rev. 138, A156 (1965).
[37]The following band structure data are used: energy gap $E_g = 812$ meV (Ref. 14); spin-orbit splitting of the valence band $\Delta_0 = 749$ meV (Ref. 15); electron mass $m_e = 0.0405\, m_0$ [D. Bimberg, W. Rühle in *Proceedings of the 12th International Conference on the Physics of Semiconductors*, Stuttgart, 1974, edited by M. Pilkuhn (Teubner, Stuttgart, 1974), p. 561]; heavy-hole mass $m_{hh} = 0.44\, m_0$ [A. Filiou and E. Fortin, Phys. Rev. B 8, 3852 (1973)]; hole mass in the split-off band $m_s = 0.15\, m_0$ (Ref. 15).
[38]J. S. Blakemore, *Semiconductor Statistics* (Pergamon, Oxford, 1962), p. 83.